frontiers | Frontiers in Earth Science

TYPE Original Research
PUBLISHED 02 February 2023
DOI 10.3389/feart.2022.1118935

OPEN ACCESS

EDITED BY
Yunhui Zhang,
Southwest Jiaotong University, China

REVIEWED BY
Miaomiao Ge,
Wenzhou University, China
Chenxi Tong,
Central South University, China

*CORRESPONDENCE
Cheng Zeng,
Cheng.Zeng@uon.edu.au

SPECIALTY SECTION
This article was submitted to Environmental Informatics and Remote Sensing, a section of the journal Frontiers in Earth Science

RECEIVED 08 December 2022
ACCEPTED 30 December 2022
PUBLISHED 02 February 2023

CITATION
Yang R, Li J, Bai X and Zeng C (2023), Stability analysis of rock slopes using the interface contact model and strength reduction method.
Front. Earth Sci. 10:1118935.
doi: 10.3389/feart.2022.1118935

Stability analysis of rock slopes using the interface contact model and strength reduction method

Rui Yang[1], JiaCheng Li[1], Xue Bai[1] and Cheng Zeng[2]*

[1]Key Laboratory of Urban Underground Engineering of Ministry of Education, Beijing Jiaotong University, Beijing, China, [2]Discipline of Civil, Surveying and Environmental Engineering, Priority Research Centre for Geotechnical Science and Engineering, The University of Newcastle, Callaghan, NSW, Australia

The assessment of rock slope stability is usually controlled by the presence of discontinuities. The block theory is an established method in practical engineering to predict the stability of rock slopes. A maximum of two discontinuity planes are considered in the application of the block theory. It would lead to inaccurate prediction of slopes with multiple discontinuity planes. A novel method for estimating the safety margin of rock slopes is proposed, which is capable of considering the contribution of all discontinuities to the stability problem. The discontinuity planes are simulated by an interface contact model within the theoretical framework of the finite difference method. The factor of safety is obtained by the strength reduction method. The failure criteria of rock slopes are also discussed. The proposed model can simulate discontinuous planes in a more realistic manner and thus is more effective in engineering practice. To demonstrate the effectiveness of the proposed model, several numerical examples are presented, which showcase its superiority for predicting the stability of blocks composed of multiple discontinuities. Several numerical examples are analyzed to confirm the effectiveness of the proposed model and its superiority in stability prediction of blocks formed by multiple discontinuities.

KEYWORDS

interface contact element, strength reduction method, stability analysis, rock slope, discontinuous deformation

1 Introduction

Rock slope stability is generally governed by the presence of discontinuities which developed in rocks. The combination of these discontinuities may result in a set of removable key blocks that significantly decrease the overall stability of slopes. It is vital to develop an effective method for evaluating the stability of key blocks for safe rock slope excavation and construction.

Extensive research studies have been conducted to investigate the stability of rock slopes. Goodman and Shi (1985) proposed the block theory to analyze the stability of the rock wedge, and it has been widely adopted in engineering because of its simplicity of concept. Chen (2004) developed a theoretical method for assessing the stability of the rock wedge based on limit equilibrium analysis. Ma et al. (2019) explored the applicability of the block theory to the wedge probability analysis by considering the variabilities of the geometric and rock properties of blocks. Deng (2021) established a spatial model of rock slopes based on the characteristics of discontinuities and slope surfaces. However, these block theory-based methods have some limitations for a general rock block formed by multiple discontinuities. The factor of safety and failure modes can be inaccurately estimated when these methods are adopted for the stability of rock blocks formed by multiple structural planes. Jiang and Zhou

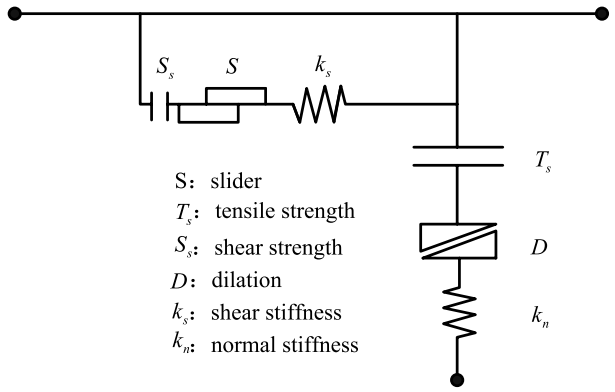

FIGURE 1
Components of the bonded interface constitutive model.

(2017) proposed a rigorous solution based on the limit equilibrium method (LEM) and kinematic analysis for the stability of polyhedral rock blocks formed by multiple discontinuities. Nevertheless, when analyzing the stability of a rock block, LEM does not completely take into account the shear forces acting on the sliding surfaces of either side of the rock block.

Zienkiewicz et al. (1975) first applied the strength reduction method (SRM) to evaluate the slope stability. Since then, some researchers have employed the SRM with finite element methods (FEMs) and finite difference methods (FDMs) to analyze the stability of slopes. The factor of safety (FS) is comparable with the result from LEM as found by Ugai and Leshchinsky (1995), Griffiths and Lane (1999), Zheng et al. (2007), and Griffiths and Marquez (2007). In comparison to the LEM, the SRM has a number of advantages including the abilities to model complex geometric and boundary conditions, the nonlinear behavior of rocks and soils, and the progressive collapse of slopes (Wei et al., 2009; Xi et al., 2014; Zhao et al., 2019). It is noted, however, most of the applications are for soil slopes. The applications of SRM to rock slopes are rare with a few exceptions including Jiang et al. (2015) and Lu et al. (2020). The existing rock slope applications of SRM involve modeling the discontinuities based on solid elements neglecting the significant disparity in the physical and mechanical characteristics of intact rocks and discontinuities. In addition, the failure criterion of the soil slope is directly applied to the rock slope despite the distinction failure mode of soil slopes and rock slopes.

In this paper, an FDM interface contact model developed for rock slopes is first introduced. The proposed model is capable of modelling discontinuities by interface contact elements, and it is reasonable considering the contribution of multiple discontinuities. The shear reduction approach is adopted to assess the stability of rock slopes. Then, the failure criterion of rock slopes is discussed. To validate the reliability of the proposed method, four typical examples are analyzed by FlAC^{3D}. The effects of the stiffness of interfaces, mesh size, and failure criteria on the *FS* and computation time are also investigated. Moreover, the proposed method is applied in the stability analysis of the right dam abutment of the Yinpan Hydropower Station in Wulong County, Chongqing Province, China. The results show that the proposed method is effective in assessing multiple structural planes.

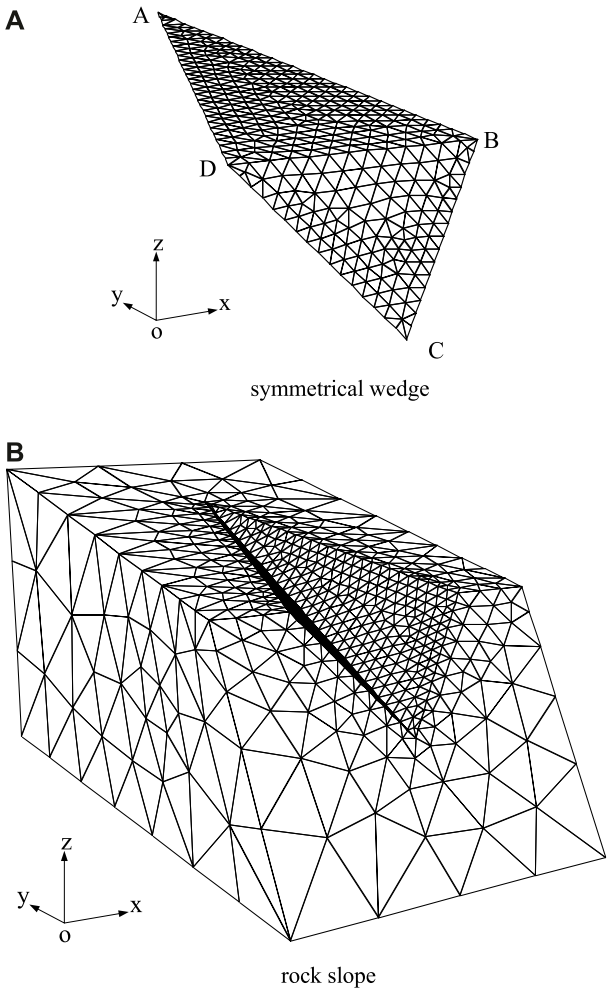

FIGURE 2
Three-dimensional mesh discretization for rock slopes with a symmetrical wedge. **(A)** Symmetrical wedge **(B)** Rock slope.

2 Methodology

2.1 Constitutive relation of the interface contact model

Advanced numerical models provide two approaches for modelling rock discontinuities: zero-thickness interface contact elements to facilitate the transmission of both shear and normal stress from the rock to the discontinuity structure planes and solid elements with finite depth. The interface contact elements in FlAC^{3D} with zero thickness are used to model the discontinuities in rock slopes.

Figure 1 illustrates the constitutive model of the interface elements. The Coulomb sliding law (Itasca 2000) is used to characterize the shear strength of the interface, which is represented by a linear Coulomb shear-strength criterion, normal and shear stiffnesses, tensile and shear bond strengths, and a dilation angle. The dilation angle is assumed to be zero in this paper, and a non-associate flow rule is used, which limits the shear force acting at an interface node and causes an increase in effective normal force on the target face after the shear-strength limit is reached.

TABLE 1 Geometrical and material parameters of example 1.

Surface	Dip direction/(°)	Dip angle/(°)	Shear strength	
			c (kPa)	ϕ (°)
Discontinuity ADC	115	45	20	20
Discontinuity ABC	245	45	20	20
Slope top surface	180	10	—	—
Slope surface	180	45	—	—

TABLE 2 Geometrical and material parameters of example 2.

Surface	Dip direction/(°)	Dip angle/(°)	Shear strength	
			c (kPa)	ϕ (°)
Discontinuity ADC	120	40	50	30
Discontinuity ABC	240	60	50	30
Slope upper surface	180	0	—	—
Slope surface	180	60	—	—

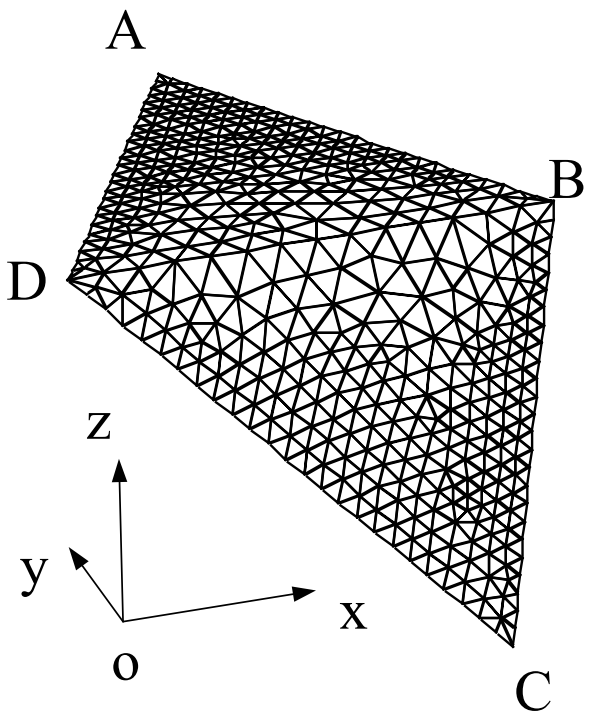

FIGURE 3
Three-dimensional mesh discretization for the asymmetrical wedge. 3) Example 3

The absolute normal penetration and the relative shear velocity of every interface node and its corresponding target face are determined at every time step. The interface constitutive model utilizes these values to generate a normal force and a shear-force vector. They are calculated at time $t + \Delta t$ as follows:

$$\begin{cases} F_n^{(t+\Delta t)} = k_n u_n A + \sigma_n A, \\ F_{si}^{(t+\Delta t)} = F_{si}^t + k_n \Delta u_{si}^{(t+\Delta t/2)} A + \sigma_{si} A, \end{cases} \tag{1}$$

where $F_n^{(t+\Delta t)}$ and $F_{si}^{(t+\Delta t)}$ are the normal force and shear force at time $t + \Delta t$, respectively; k_n and k_s denote the normal and shear stiffnesses, respectively; u_n is the absolute normal penetration of the interface node into the target face; Δu_{si} is the incremental relative shear displacement; σ_n is the additional normal stress that is generated as a result of interface stress initialization; σ_{si} is the extra shear stress that results from the interface stress initialization; and A is an area that is associated with the node in the contact model.

The Coulomb shear-strength criterion restricts the magnitude of the shear force according to a specific equation.

$$F_{s\max} = cA + \tan\varphi\left(F_n - pA\right), \tag{2}$$

where $F_{s\max}$ is the maximum shear force, c is the cohesion along the interface, φ is the friction angle of the interface surface, and p is the pore pressure (interpolated from the target face). The sliding along the interface shall occur when the criterion $|F_s| \geq F_{s\max}$ is fulfilled. The shear force should be adjusted to the maximum shear stress ($|F_s| = F_{s\max}$), and the direction remains unchanged.

If either the shear stress is greater than the shear strength or the tensile effective normal stress is more than the normal strength, the bond will be broken. Then the normal force and shear force turn to be zero. The interface elements can well simulate the deformation and stress characteristics of the discontinuous plane.

The intercalation capacity of two contact surfaces is determined by normal stiffness k_n and shear stiffness k_s. The analysis is significantly influenced by the interface shear and normal stiffnesses. The bigger the stiffness, the more difficult it is to penetrate between two contact surfaces. Utilizing stiffnesses of a high magnitude will result in a slow convergence rate of the solution (Rosso, 1976; Bandis et al., 1983). The equivalent stiffness proposed by Fossum (1985) for a zone in the normal direction can be determined as follows:

TABLE 3 Geometrical and material parameters of example 3.

Surface	Dip direction/(°)	Dip angle/(°)	Shear strength	
			c (kPa)	ϕ(°)
Discontinuity ABED	225	50	150	30
Discontinuity ACFD	150	45	150	30
Discontinuity ABC	180	30	20	30
Slope upper surface	180	0	—	—
Slope surface	180	60	—	—

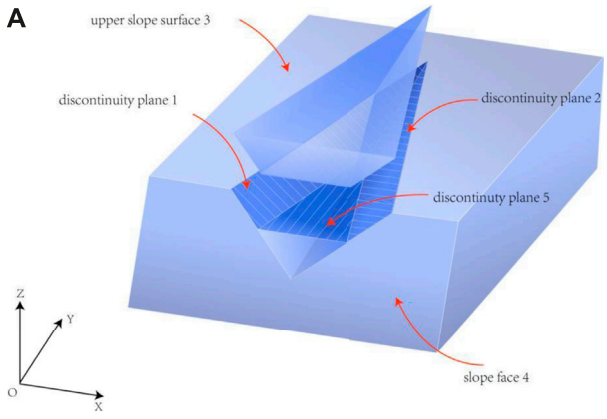

Geometry of a typical movable block forming by three discontinuities

FIGURE 4
Three-dimensional model for example 3 **(A)** Geometry of a typical moveable block forming by three discontinuities. **(B)** Vertical view of the movable block.

$$k_e = \frac{K + 4G/3}{\Delta z_{\min}}, \tag{3}$$

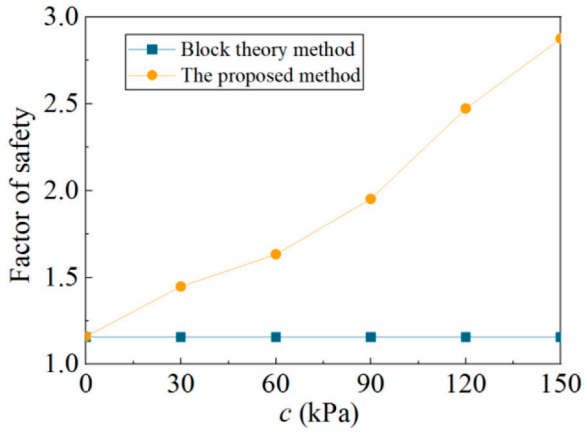

FIGURE 5
Effect of the cohesion of discontinuities ABED and ACFD on slope stability analysis. 4) Example 4

where k_e is the equivalent stiffness; K and G are the bulk and shear moduli, respectively; and $\Delta z_{\min}$ is the smallest width in the normal direction of an adjoining zone. To join two sub-grids, the interface must be utilized with the higher shear and normal stiffnesses than the equivalent stiffness (k_s and k_n higher than k_e) to prevent any movement.

2.2 Strength reduction method

The strength reduction finite difference method is proposed to predict the stability of a rock slope. The SRM is intended to reduce the cohesion c_j and internal friction angle $\tan\phi_j$ of rock discontinuities progressively until the critical failure state, as described in the next section, is reached. The shear strength parameters $c_j^{'}$ and $\phi_j^{'}$, which have been factored, are represented by

$$c_j^{'} = \frac{c_j}{SRF}, \tag{4}$$

$$\phi_j^{'} = \arctan\left(\frac{\tan\phi_j}{SRF}\right), \tag{5}$$

where SRF is the strength reduction factor. When the critical state is determined, the factor of the safety of the rock slope is the same as SRF

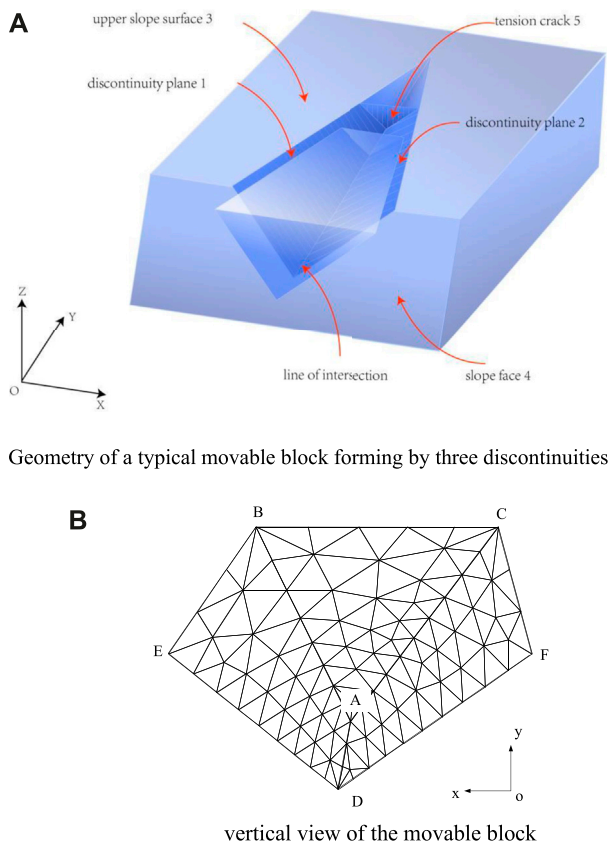

FIGURE 6
Three-dimensional model for example 4. **(A)** Geometry of a typical movable block forming by three discontinuities. **(B)** Vertical view of the movable block.

and $FS = SRF$. Therefore, the failure criteria directly influence the value of FS.

2.3 Failure criteria in strength reduction for rock slopes

The failure criteria for evaluating if a soil slope has reached its critical state have been widely discussed. The most widely used failure criteria for soil slopes are presented as follows.

1) Strain and displacement mutation of specific points.

2) The non-convergence of a numeral model computation.
3) Plastic shear strain runs through the slope.

Using the displacement mutation of specific points as failure criteria is not objective enough due to specific points' selection and the determination of whether the displacement mutation of these points depends on subjective judgment. The convergence speed of a numeral model is influenced by grid partitioning. The occurrence of a plastic zone stretching from the bottom to the top of a slope does not necessarily signify slope failure.

Research studies on the failure criteria of rock slopes are rare. Most of the researchers adopted failure criteria for soil slopes to obtain the FS of rock slopes. The assessment of FS based on soil slope failure criteria could give a misleading conclusion regarding the rock slope stability. It is assumed that the critical state is reached when all the nodes of interface contact elements are either sliding or opening, as the rock slope stability is generally governed by multiple structural planes. The new failure criteria are more effective in depicting the failure behavior of a rock mass.

3 Examples

The stability assessment of a rock slope that includes either a wedge formed by two discontinuities or a pentahedron formed by three discontinuities is of great interest in rock slope engineering. To verify the effectiveness of the proposed method, four rock slope examples are analyzed by the traditional method and proposed method. The analysis is carried out using the high-performance laptop with Intel(R) Core(TM) i7-10875H CPU @ 2.30 GHz. The movable block in examples 1 and 2 is formed by two discontinuities, while that in examples 3 and 4 is formed by three discontinuities.

1) Example 1: Symmetrical wedge

The first problem deals with a symmetrical wedge with two discontinuities, as illustrated in Figure 2. The rock slope surface of this wedge has an inclination of 45° with a dip direction of 185°, while the upper surface of slope dips has an inclination of 10° with a dip direction of 180°. The wedge has a height of 64.89 m and is intersected by two discontinuities (i.e., ADC and ABC). Details of discontinuities for geometry and geotechnical properties are given in Table 1. The unit weight is $\gamma = 26\text{kN/m}^3$, the bulk modulus is $K = 10$ GPa, and the elastic modulus is $G = 3$ GPa. The discontinuities are modelled by interface contact elements comprising 456 nodes and 818 elements.

TABLE 4 Geometrical and material parameters of example 4.

Surface	Dip direction/(°)	Dip angle/(°)	Shear strength	
			c (kPa)	ϕ(°)
Discontinuity ABED	235	45	20	30
Discontinuity ACFD	105	45	20	30
Discontinuity ABC	180	45	20	30
Slope upper surface	180	0	—	—
Slope surface	180	60	—	—

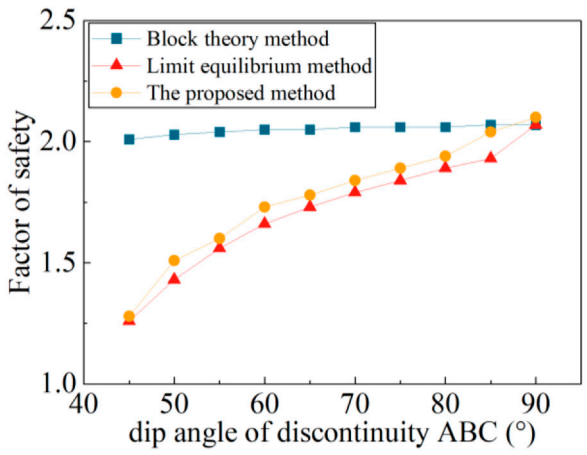

FIGURE 7
Effect of the dip angle of discontinuity ABC on slope stability analysis.

TABLE 5 Effects of k_s, k_n on the *FS* and computation time for wedges.

Symmetrical wedge			Asymmetrical wedge		
k_s, k_n	*FS*	Time step	k_s, k_n	*FS*	Time step
k_e	1.310	4921	k_e	1.643	9065
10 k_e	1.316	8595	10 k_e	1.644	30,856
50 k_e	1.315	16,090	50 k_e	1.642	46,141
80 k_e	1.314	19,219	80 k_e	1.642	69,341
100 k_e	1.314	20,587	100 k_e	1.642	79,765

The obtained rock mass consisted of 1161 nodes and 4508 elements. The tetrahedron mesh of the symmetrical wedge is shown in Figure 2.

Through the procedure of shear strength reduction on the discontinuities ADC and ABC, the *FS* can be determined. When *SRF* attains 1.316, all the nodes of interface contact elements are either sliding or opening and the limit failure state is reached. For this example, the *FS* is 1.316. For comparison, the block theory is also undertaken to evaluate the stability of this example. According to the principles of the block theory, the movable block is determined to be sliding along the juncture where two sliding surfaces intersect. The block theory derived closed-form equations for this failure mode to calculate the *FS*. The *FS* has an exact value of 1.293. It was found that *FS* estimated by the proposed method is consistent with the block theory, which is proved to be an accurate method for evaluating stability of symmetrical wedges. Thus, the rationality and effectiveness of the proposed method have been demonstrated.

2) Example 2: Asymmetrical wedge

Example 2 consists of an asymmetrical wedge with two discontinuities ADC and ABC. The shear strength and geometric features of the example are provided in Table 2. In this case, the rock unit weight is $\gamma = 26\text{kN/m}^3$, the bulk modulus is $K = 10$ GPa, and the elastic modulus is $G = 3$ GPa. FLAC^{3D} is employed to develop a numerical model of the rock slope. Figure 3 shows the tetrahedron mesh of the asymmetrical wedge with 256 nodes and 451 interface contact elements The obtained rock mass consisted of 632 nodes and 2350 elements. Both the proposed method and block theory-based method are employed to evaluate the stability of this example. The *FS* obtained by the proposed method is 1.644, which is very close to the result (*FS*=1.640) estimated by the block theory. The effectiveness of the proposed method is further confirmed.

Example 3 is a rock slope with a movable block formed by three discontinuity surfaces (ABED, ACFD, and ABC) as shown in Figure 3A. In this case, the volume of the block is 6076 m^3. The area of structural surfaces ABED, ACFD, and ABC is 573 m^2, 878 m^2, and 81 m^2, respectively. The strengths and orientations of the three discontinuities are given in Table 3. The rock unit weight is $\gamma = 26\text{kN/m}^3$, the bulk modulus is $K = 10$ GPa, and the elastic modulus is $G = 3$ GPa. Discontinuities are simulated using interface contact elements within the theoretical framework of the finite difference method. The tetrahedron mesh of the rock block is shown in Figure 3B. The mesh of the interface comprised 69 nodes and 106 elements.

The *FS* for this example is obtained by the proposed method and block theory. When *SRM* is equal to 2.875, as shown in Figure 4, all the nodes of interface contact elements are either sliding or opening and the limit failure state is reached. For this problem, the *FS* is 2.875. The sliding mode of this example determined by the block theory is the single plane sliding (along ABC). In the estimation, the block theory only considers the normal and shear stresses of the sliding surface, ignoring the influence of other discontinuities. The *FS* estimated by the block theory is 1.156. It is shown that the block theory method seriously underestimates the rock slope's stability.

TABLE 6 Effects of element size of interface contact elements on the *FS*.

Symmetrical wedge				Asymmetrical wedge			
Element size	Number of elements	*FS*	Computational cost (s)	Element size	Number of elements	FS	Computational cost (s)
$l_1/50$	1562	1.320	170	$l_2/50$	2321	1.642	240
$l_1/40$	1098	1.315	106	$l_2/40$	1754	1.640	210
$l_1/30$	818	1.316	48	$l_2/30$	912	1.640	60
$l_1/20$	308	1.317	15	$l_2/20$	451	1.644	25

Notes: l_1 and l_2 are the lengths of intersection for symmetrical and asymmetrical wedges, respectively.

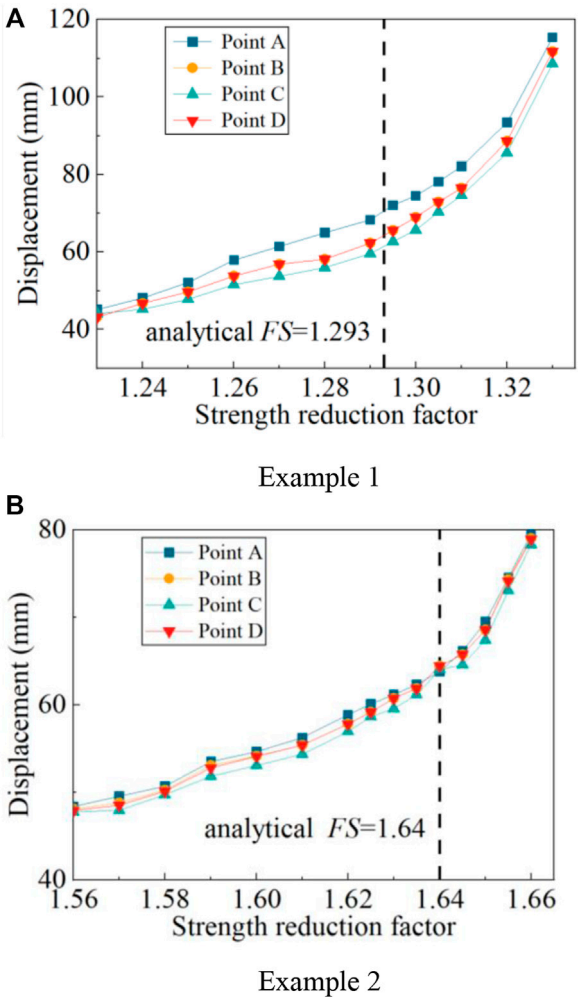

FIGURE 8
Displacement of specific points with the rise in the strength reduction factor. **(A)** Example 1 **(B)** Example 2.

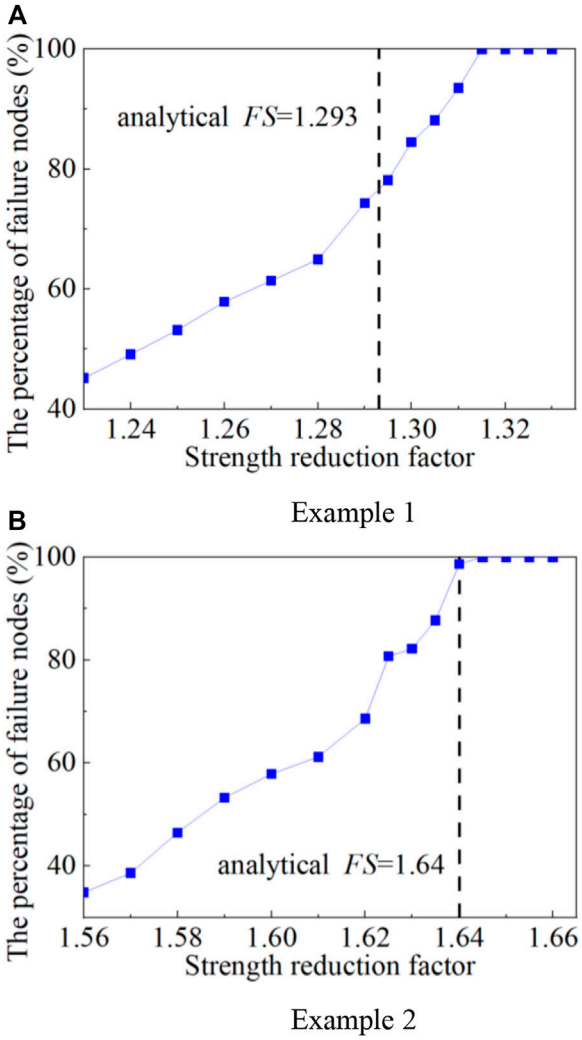

FIGURE 9
Percentage of failure nodes with the increase in the strength reduction factor. **(A)** Example 1 **(B)** Example 2.

To investigate the influence of discontinuities ABED and ACFD on the slope stability assessment, the *c* of these two planes is varied in the range of 0–150 kPa, while all other parameters remain unchanged as described in this section. For comparison, the proposed method and block theory method are carried out to estimate *FS*. The obtained results from both methods pertaining to *c* of discontinuities ABED and ACFD are demonstrated in Figure 5. It is evident that discontinuities ABED and ACFD have significant impact on the slope stability. The contribution of these structural planes is omitted by the block theory which will result in the underestimation of *FS*. The proposed method which considers the shear strength on all discontinuities would yield accurate results for rock slopes controlled by three discontinuities.

Figure 6 shows an example of a rock slope with three discontinuities developed in the rock mass. Figure 6A exhibits a tetrahedron mesh of the pentahedron. The mesh of the interface comprised 116 nodes and 172 elements. The shear strength characteristics and geometry of discontinuities are listed in Table 4. In this case, the potentially unstable block formed by the spatial intersection of discontinuities ABED, ACFD, and ABC has a volume of 10,870 m^3. The area of structural surfaces ABED, ACFD, and ABC is 683 m^2, 580 m^2, and 764 m^2, respectively.

For comparison and validation, the block theory, the three-dimensional LEM implemented using 3D slope software, and the proposed method are adopted to analyze the stability of the example rock slope. The *FS* of 1.28 obtained by the proposed method shows good agreement with that predicted by LEM (*FS*=1.26). Within the framework of the block theory, it is essential to first evaluate the failure mode. The example slope sliding direction is congruent with the junction of the two failure planes (ABED and ACFD) on the horizontal projection. The *FS* obtained from the block theory only considers normal and shear stresses of the two sliding surfaces, ignoring the influence of the tension crack. The *FS* is found to be 2.01, which overestimated the stability of the slope.

The effect of the tension crack (i.e., discontinuity ABC) on the stability of the example slope has been discussed by varying the dip angle. As depicted in Figure 7, when the tension crack dip angle is 90°, the difference in the *FS* obtained by the proposed method, block theory, and LEM is negligible. This indicates that the tension crack

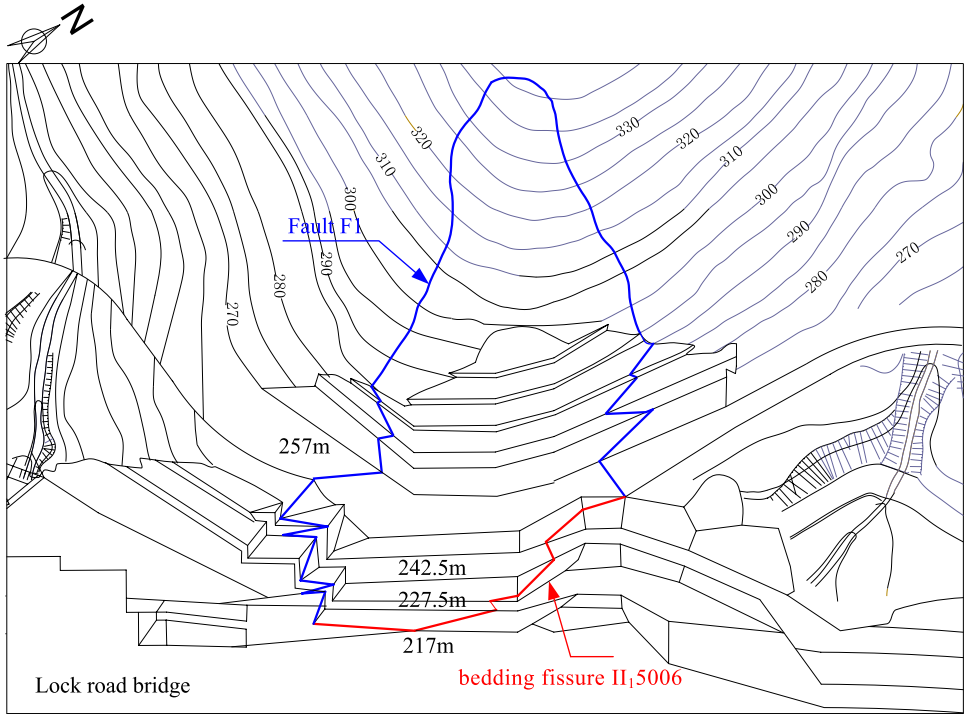

FIGURE 10
Plan layout of excavation on the right dam slope.

barely influences the analysis of slope when the dip angle is equal to 90°. It can also be found from Figure 7 that the *FS* calculated by the block theory increases slightly with the increasing tension crack dip angle. The varied volume of movable blocks and areas of sliding surfaces leads to minor difference in *FS* for different dip angles. The difference between the proposed method and block theory is increased with the decreasing tension crack dip angle. When the dip angle is equal to 45°, the relative difference in *FS* between the proposed method and block theory is 36.5%. The block theory can lead to inaccurate outcomes due to ignoring the tension crack of unstable slopes, thus overestimating the stability of slopes. The proposed method and LEM can consider the roles of all the structural planes in the stability problem, which provides a new and effective way of solving the stability problem of movable blocks. The *FS* calculated by these two methods is very close. To accurately assess the stability of rock slopes, the shear strength of all discontinuities should be considered, and their unfavorable effects on the rock stability assessment should also be reflected for calculating the *FS*.

4 Discussion

4.1 Effects of shear and normal stiffnesses on slope stability analysis

The discontinuities developed in rocks are simulated by interface contact elements. To analyze the impact of normal and shear stiffnesses on the stability of a slope, the symmetrical wedge and asymmetrical wedge are adopted and analyzed. The bulk and shear moduli of the rock mass were set at $K = 10$ GPa and $G = 3$ GPa, respectively, while k_s and k_n varied in the range of $k_e \sim 100k_e$. The effects of stiffness on the *FS* and time steps for estimating the stability of the wedges are shown in Table 5.

For the illustrative examples, although the values of stiffnesses are different, the values of *FS* are very similar. If normal stiffness k_s and shear stiffness k_n of interface contact elements are less than ten times that of k_e of adjacent zones, these stiffnesses have no influence on the estimation of *FS* and computational efficiency. If the ratio between k_s and k_e is much more than ten, the computational cost will be significantly increased. Careful consideration should be given to improve computational efficiency. It is recommended that the stiffness of a zone (k_s; k_n) should be set to ten times the stiffness of the stiffest adjacent zone.

4.2 Effects of element size on slope stability analysis

To discuss the effects of size of the interface contact element on the estimation of rock slope stability, various element sizes are utilized in the analysis. To discretize symmetrical and asymmetrical wedges, four different element sizes are employed. k_s and k_n of these two examples are set to ten times that of k_e. The results of *FS* corresponding to different element sizes are presented in Table 6. The estimation of *FS* appears to remain unchanged regardless of the size of the element. The proposed method can reach the high level of precision even when the large element size is adopted. As the number of elements increases, the computational cost also increases. To maximize efficiency, it is advisable to use a small number of elements for the proposed method.

TABLE 7 Physical and mechanical parameters of the rock mass for the right dam abutment slope.

Material	Unit weight/kN/m^3	Deformation modulus/GPa	Poisson's ratio	Shear strength	
				tan ϕ	c/MPa
S_{1ln}	25.1	6.0	.28	1.01	.81
O_{2+3}	26.5	12.5	.23	1.10	1.00
O_{1d}	27.0	11.0	.20	1.11	1.13
II_1-5006	—	—	—	.75	.50
F_1	—	—	—	.35	.05

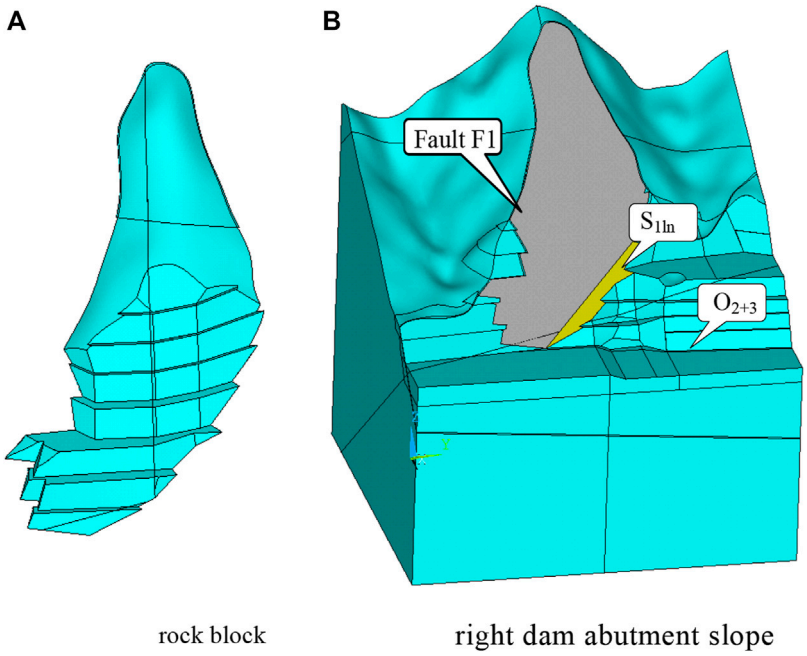

FIGURE 11
Three-dimensional model for the right dam abutment slope after excavation. **(A)** Rock block **(B)** Right dam abutment slope.

4.3 Effects of failure criteria on slope stability analysis

To investigate the effects of different criteria on the rock slope stability, both displacement mutation criterion and the proposed failure criterion (all the nodes of interface contact elements are either sliding or opening) are used to obtain the *FS* of the rock slope for examples 1 and 2. The displacements of four points (A, B, C, and D) are recorded with the rise in *SRF* as illustrated in Figure 8. The displacements of all selected points increased with the rise in *SRF*. The analytical *FS* (estimated by the block theory) of example 1 is 1.293. The displacement mutation phenomenon has not been easily observed with the increasing strength reduction. When the shear strength reduction method is applied with the displacement mutation as the slope failure criteria, the estimation of *FS* involved subjectivity. As shown in Figure 9, the number of failed nodes is increased with the increasing *SRF*. The turning points are found when *SRF*=1.316 of example 1. All the nodes of interface contact elements are either sliding or opening when *SRF*=1.316. Thus, *FS* is 1.316 according to the failure criteria. The turning points of example 2 can also be obtained when *SRF*=1.644. The results show that the *FS* estimated in the strength reduction method by the new failure criteria has good agreement with the block theory. The interface element node failure criteria are recommended for examining the stability of rock slopes because of its objectivity and clear concept.

5 Engineering application

The Yinpan Hydropower Station is situated in Wulong County, Chongqing Province, China, which is 4 km downstream from Jiangkou Town. The Yinpan Hydropower Station, as the 11th cascade development on the main stream of the Wujiang River, is a comprehensive hydro-project designed for electric power

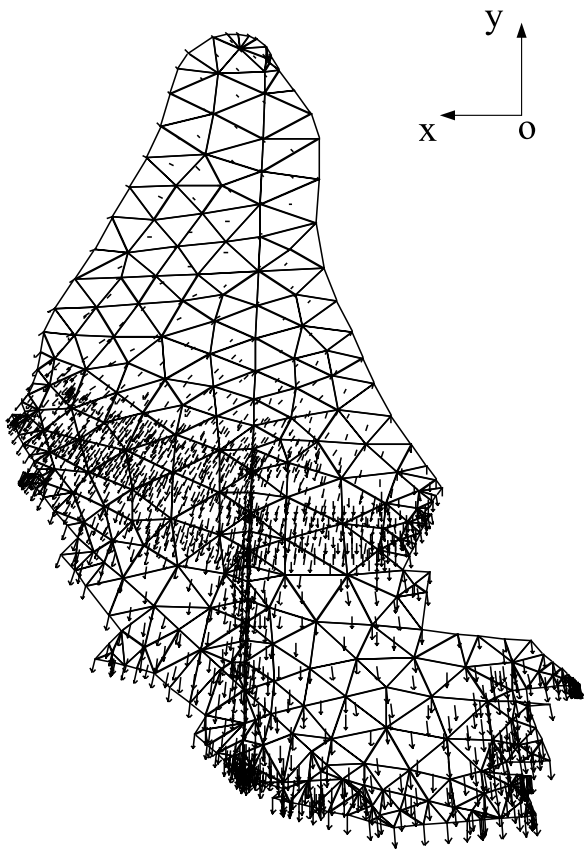

FIGURE 12
States of interface nodes for the rock block of the right dam slope.

generation in combination with navigation. The hydropower station includes the construction of a 653.8-m-long and 80-m-high concrete gravity dam.

The gradient of natural rock slopes on the right bank is about 35°. The rock of the slope is composed of S_{ln}^{1} shale, O_{3w} shale, O_{2+3} limestone, O_{1d} sandstone, and shale from the top to bottom. Figure 10 depicts the geological plan layer of excavation on the right abutment slope. As indicated in the field geological investigation and geological survey of the right bank, there is a latent large block generated by fault F_1 and bedding fissure II_15006 that developed in S_{ln}^{1} shale, as shown in Figure 10. The intersection angle between F_1 and slope strike is about 12°. The altitude of fault F_1 is 110°∠38°. The composition of fault F_1 is muddy intercalation within broken shale. The broken rock has a diameter of 5–15 cm and a general width of .5–3 cm. After excavation, the lower part of fault F_1 exposure led to right abutment slope failure. The altitude of bedding fissure II_15006 is 272°∠41° whose joint connectivity is 20% consisting of the calcite membrane. According to the engineering geological investigation, the physical and mechanical properties of the dam abutment slope and the shear strength parameters of the slip surfaces are listed in Table 7.

A model is built to analyze the *FS* after excavation based on the geological reveals in the right slope. The numerical model for the right dam abutment slope is presented in Figure 11. The numerical model is composed of 1161 nodes and 4508 elements. The volume of the potential failure block is 21,445 m3. Fault F1 and bedding fissure II_15006 are simulated by interface contact elements within the theoretical framework of the finite difference method. The mesh of the interface comprised 402 nodes. For the right dam abutment slope, the *SRF* is 1.04 when all the nodes of interface contact elements are either sliding or opening. Therefore, the *FS* is 1.04. Figure 12 shows the states of interface nodes with different reduction factors of shear

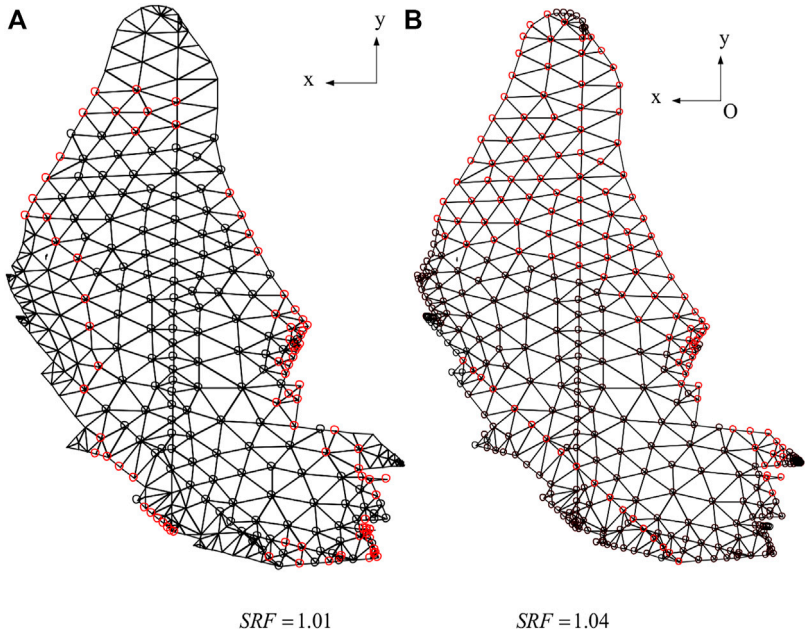

FIGURE 13
Sliding direction vectors of the dam slope at the critical state **(A)** SRF=1.01 **(B)** SRF=1.04.

strength. Circles at nodes represent that the interface has slipped in the shear or normal direction. Red circles represent opening contact nodes, and black circles represent sliding contact nodes. Figure 13 represents the plane sliding direction vectors of the right dam abutment slope at a critical state.

The failure mode of right slopes obtained by the block theory is single plane sliding with fault F_1. When considering a potential sliding of the right dam slope along fault F_1, a unique decomposition of forces on the sliding body is induced into a component along the sliding direction and a component perpendicular to the sliding direction. Thus, the *FS* obtained from the block theory is .72. However, when the block fails, II_15006 would resist sliding of the movable block and change the sliding direction. Since the block theory method ignores the role of bedding fissure II_15006, the block theory underestimated the stability of the right dam abutment slope. The proposal method can consider roles of all the structural planes in the stability problem and obtain credible results Figure 13.

6 Conclusion

In order to analyze rock slopes with multiple discontinuities, which can induce ill-advised results by the conventional block theory, this paper proposes a method for estimating the *FS* of complex blocks, in which the discontinuities are simulated by interface contact elements within the theoretical framework of the finite difference method based on the strength reduction method. The effects of shear and normal stiffnesses, element size of wedges, and failure criteria on the stability analysis were further investigated by the proposal method. The following conclusions can be drawn from the results and discussion of this paper:

1) The validity of the proposed model is demonstrated by some typical examples of wedges. For wedge examples, the *FS* values calculated by the proposed method are consistent with the traditional method. For the stability analysis of blocks formed by multiple structural planes, the proposed method can consider roles of all the structural planes in the stability problem. Thus, the proposed method provides engineers with a practical method for 3D jointed rock slope stability analysis.
2) The stiffnesses of the interface contact element and element size have no influence on the estimation of *FS*. However, large values of stiffnesses and small element size will result in low computational efficiency. Therefore, it is of great importance for adopting the suitable stiffnesses of the interface element and element size to improve solution efficiency. The failure criteria of the interface contact node provide a more accurate way to indicate the failure behavior of a rock slope.
3) The proposed method is utilized to assess the stability of the Yinpan Hydropower Station right abutment slope. The traditional block theory method fails to accurately assess the stability of the slope due to its inability to consider the contributions of all the structural planes. However, the proposed method takes into account all the structural planes and produces more reliable results.

Data availability statement

The original contributions presented in the study are included in the article/Supplementary Material; further inquiries can be directed to the corresponding author.

Author contributions

RY: methodology, software, validation, investigation, formal analysis, data curation, writing—original draft, writing—review and editing, and visualization. CZ: conceptualization, methodology, software, validation, formal analysis, writing—original draft, writing—review and editing, visualization, supervision, and project administration. JL: software, validation, and writing—review and editing. XB: software, validation, and writing—review and editing.

Funding

This study was supported by the Fundamental Research Funds for the Central Universities (2021JBM037) and the China Postdoctoral Science Foundation project (2022M710341).

Conflict of interest

The authors declare that the research was conducted in the absence of any commercial or financial relationships that could be construed as a potential conflict of interest.

Publisher's note

References

Bandis, S. C., Lumsden, A. C., and Barton, N. R. (1983). Fundamentals of rock joint deformation. *Int. J. Rock Mech. Min.* 20 (6), 249–268. doi:10.1016/0148-9062(83)90595-8

Chen, Z. (2004). A generalized solution for tetrahedral rock wedge stability analysis. *Int. J. Rock Mech. Min. Sci.* 41 (4), 613–628. doi:10.1016/j.ijrmms.2003.12.150

Deng, D. (2021). Limit equilibrium analysis on the stability of rock wedges with linear and nonlinear strength criteria. *Int. J. Rock Mech. Min. Sci.* 148, 104967. doi:10.1016/j.ijrmms.2021.104967

Fossum, A. F. (1985). Effective elastic properties for a randomly jointed rock mass. *Int. J. Rock Mech. Min. Sci. Geomechanics Abstr.* 22 (6), 467–470. doi:10.1016/0148-9062(85)90011-7

Goodman, R. E., and Shi, G. H. (1985). *Block theory and its application to rock engineering*. USA: Prentice-Hall.

Griffiths, D. V., and Lane, P. A. (1999). Slope stability analysis by finite elements. *Geotechnique* 49, 387–403. doi:10.1680/geot.1999.49.3.387

Griffiths, D. V., and Marquez, R. M. (2007). Three-dimensional slope stability analysis by elasto-plastic finite elements. *Geotechnique* 57 (6), 537–546. doi:10.1680/geot.2007.57.6.537

Itasca, F. (2000). *Fast Lagrangian analysis of continua*. Minneapolis, Minn: Itasca Consulting Group Inc.

Jiang, Q., Qi, Z., Wei, W., and Zhou, C. (2015). Stability assessment of a high rock slope by strength reduction finite element method. *Bull. Eng. Geol. Environ.* 74 (4), 1153–1162. doi:10.1007/s10064-014-0698-1

Jiang, Q., and Zhou, C. (2017). A rigorous solution for the stability of polyhedral rock blocks. *Comput. Geotechnics* 90, 190–201. doi:10.1016/j.compgeo.2017.06.012

Lu, R., Wei, W., Shang, K., and Jing, X. (2020). Stability analysis of jointed rock slope by strength reduction technique considering ubiquitous joint model. *Adv. Civil Eng.*, 1–13. doi:10.1155/2020/8862243

Ma, Z., Qin, S., Chen, J., Lv, J., Chen, J., and Zhao, X. (2019). A probabilistic method for evaluating wedge stability based on blind data theory. *Bull. Eng. Geol. Environ.* 78 (3), 1927–1936. doi:10.1007/s10064-017-1204-3

Rosso, R. S. (1976). A comparison of joint stiffness measurements in direct shear, triaxial compression, and *in Situ*. *Int. J. Rock Mech. Min. Sci. Geomechanics Abstr.* 13 (6), 167–172. doi:10.1016/0148-9062(76)91282-1

Ugai, K., and Leshchinsky, D. (1995). Three-dimensional limit equilibrium and finite element analyses: A comparison of results. *Soils Found.* 35 (4), 1–7. doi:10.3208/sandf.35.4_1

Wei, W. B., Cheng, Y. M., and Li, L. (2009). Three-dimensional slope failure analysis by the strength reduction and limit equilibrium methods. *Comput. Geotechnics* 36 (1–2), 70–80. doi:10.1016/j.compgeo.2008.03.003

Xi, C., Wu, Y., Yu, Y., Liu, J., Xi, F. X., and Ren, J. (2014). A two-grid search scheme for large-scale 3-D finite element analyses of slope stability. *Comput. Geotechnics* 62, 203–215. doi:10.1016/j.compgeo.2014.07.010

Zhao, M., Guo, W., Chen, L. Y., and Wang, S. Y. (2019). Experiment on the frost resistance of modified phospho gypsum: A case used to improve baozhong railway subgrade loess. *J. Mt. Sci.* 16 (12), 2920–2930. doi:10.1007/s11629-018-5014-2

Zheng, Y., Deng, C., Zhao, S., and Tang, X. (2007). Development of finite element limiting analysis method and its applications in geotechnical engineering. *Sciences* 2007 (3), 10–36.

Zienkiewicz, O. C., Humpheson, C., and Lewis, R. (1975). Associated and non-associated visco-plasticity and plasticity in soil mechanics. *Geotechnique* 25 (4), 671–689. doi:10.1680/geot.1975.25.4.671